



ISSN: 2319-5967

ISO 9001:2008 Certified

International Journal of Engineering Science and Innovative Technology (IJESIT)

Volume 7, Issue 4, July 2018

ENTROPY ANALYSIS OF UNSTEADY MIXED CONVECTION BOUNDARY LAYER FLOW OF MAGNETO-NANOFUID PAST A VERTICAL INFINITE PLATE

M. M. Wafula, M.N. kinyanjui, P.R Kiogora

Abstract: Magneto hydrodynamics boundary layer flow of unsteady laminar nanofluids over an accelerating convectively heated vertical plate and heat transfer are numerically studied. Three different types of water-based Nanofluids containing Titanium (iv) oxide, Copper and aluminum (iii)oxide are taken into consideration. The governing equations are solved numerically by shooting technique coupled with Runge-Kutta-Fehlberg integration scheme. The expression for entropy generation number and the Bejan number are obtained based on the profiles. A comparison of the entropy generation due to the heat transfer and the fluid friction is made with the help of the Bejan number. It is observed that the presence of the metallic nanoparticles creates more entropy in the nanofluid flow than in the regular fluid flow.

Index terms: Nanofluids, Mixed convection, Unsteady MHD flows, Entropy generation, Bejan number.

I. INTRODUCTION

Most conventional heat transfer fluids, such as water, engine oil and Ethylene Glycol are restricted in terms of thermal properties are restricted in terms of thermal properties, which in turn, may have limited applications in heat transfer industries. Although various techniques have been used to enhance their heat transfer, their performance is often limited by their low thermal conductivities which hinder the performance enhancement and compactness of heat exchangers. With the rising demands of modern technology for process intensification and device miniaturization, there is need to develop new types of fluids that are more effective in terms of heat exchange performance. In order to achieve this, researchers proposed to disperse small amounts of nanometer-sized (10-50nm) solid particles (nanoparticles) in base fluids, resulting into what is commonly known as nanofluids. Nanofluids were first introduced by Choi [1]. Investigations have shown that nanofluids possess enhanced thermo physical properties such as thermal diffusivity, thermal conductivity, convective heat transfer coefficients and viscosity compared to those of base fluids like oil or water [2]. Nanofluids have a wide range of applications, ranging from transportation to energy production. In this era of energy saving and the widespread use of battery operated devices, such as laptops and cellphones, a smart technological handling of energetic resources is necessary. Nanofluids have played this role perfectly. They can be used as a smart material, working as a heat valve to control the heat flow. With the application of magnetic field, nanofluids has several applications, and may be used to deal with the problems such as cooling nuclear reactors by liquid sodium and inducing the flow meter which depends on the potential difference in the fluid along the direction perpendicular to the motion and to the magnetic field. Examples of how nanotechnology may be integrated into each of these technological areas are highlighted in the following specific applications as stated by Routbort [3], among others.

Mixed convection flows is a combined forced and free convection flows. Such processes occur when the effects of buoyancy forces in forced convection or the effects of forced flow in free convection become significant. Forced and free convection is especially pronounced in situations where the forced flow velocity is low and/or the temperature differences are large. This type of flows are frequently experienced in many transport and in engineering sectors such as manufacture and extraction of polymer and rubber sheets, paper production, wire drawing and glass-fiber production, melt spinning, continuous casting, heat exchangers, solar collectors, nuclear reactors and in electronic equipment, Tadmor [4]. The steady mixed convection boundary layer flow on a vertical surface without the effect of viscous dissipation was studied by Dey and Nath [5]. Xu et al [6] have analyzed the mixed convection flow of a nanofluid in a vertical channel. Fan et al. [7] investigated mixed convection heat transfer in a horizontal channel filled with nanofluids. One of the major concerns of engineers is to find ways which

could control the wastage of useful energy; mostly in thermo dynamical systems, energy losses can cause great disorder. This disorder in the system is measured in terms of energy. The optimal design for any thermal system can be achieved by minimizing entropy generation in the systems. The analysis of the energy utilization and the entropy generation has become one of the primary objectives in designing a thermal system. Bejan [8] has explained the systematic methodology of calculating entropy generation through heat and fluid flow in heat exchangers. Butt and Ali [9] carried out entropy analysis of the flow and heat transfer caused by a moving plate. The equations that govern the flow and heat transfer phenomenon were solved numerically. Arikoglu et al [10] examined the effect of slip on entropy generation in Magneto dynamics (MHD) flow over single rotating disc. Makinde [11] examined the entropy generation on an MHD flow and heat transfer over a flat plate with the convective boundary condition. Narusawa [12] and Rosen [13] have presented fundamentals of entropy generation. Much has been done numerically and experimentally on studies involving nanofluids with different geometries and boundary conditions, only few of them considered an accelerated vertical plate. This study analyzes the engineering processes in which energy losses can significantly reduce efficiency or cause much damage. The solutions are obtained numerically, and the results are discussed and analyzed using graphs.

II. MATHEMATICAL FORMULATION

Consider the mixed convection unsteady MHD boundary layer flow past a vertical plate as shown in figure 1. A Cartesian co-ordinate system is chosen with x-axis vertically upwards along the direction of the flow and y-axis is normal to the surface of the plate. The plate moves with velocity $U_w(x, t)$, and the left side of the plate is heated by convection from a hot fluid at temperature $T_w(x)$, while the temperature of the ambient cold fluid is T_∞ with a heat transfer coefficient h_f . For the time $t = 0$, the fluid is steady. The unsteady fluid start at $t > 0$. A transverse

magnetic field of strength $B = B_0(1 - ct)^{\frac{1}{2}}$ is applied parallel to the y-axis. It is also assumed that the induced magnetic field is negligible in the flow field in comparison with the applied magnetic field. The flow is stable and all body forces except magnetic field are neglected. The thermo-physical properties of the nanofluid are given in Table 1.

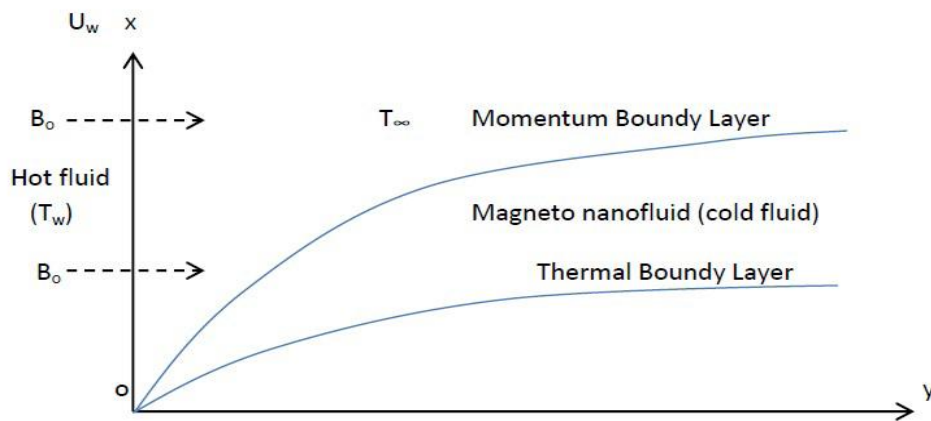


Fig 1: Geometry of the problem

Under the above assumptions, the continuity, momentum and energy equations describing the flow are written as

$$\frac{\partial u}{\partial x} = 0 \quad (1)$$

$$\frac{\partial u}{\partial t} + u \frac{\partial u}{\partial x} + v \frac{\partial u}{\partial y} = -\frac{1}{\rho_{nf}} \frac{\partial p}{\partial x} + \frac{\mu_{nf}}{\rho_{nf}} \left(\frac{\partial^2 u}{\partial y^2} \right) + g\beta_{nf}(T - T_f) - \frac{\sigma_{nf} B_0^2 u}{\rho_{nf}} \quad (2)$$



ISSN: 2319-5967

ISO 9001:2008 Certified

International Journal of Engineering Science and Innovative Technology (IJESIT)

Volume 7, Issue 4, July 2018

$$\frac{\partial T}{\partial t} + u \frac{\partial T}{\partial x} + v \frac{\partial T}{\partial y} = \frac{k_{nf}}{(\rho C_p)_{nf}} \frac{\partial^2 T}{\partial y^2} + \frac{\mu_{nf}}{(\rho C_p)_{nf}} \left(\frac{\partial u}{\partial y} \right)^2 + \frac{\sigma_{nf} B_0^2 u^2}{(\rho C_p)_{nf}} \quad (3)$$

Where u and v are the velocity components along the x and y -directions respectively, T is the temperature of the nanofluid, μ_{nf} the dynamic viscosity of the nanofluid, ρ_{nf} the density of nanofluid, σ_{nf} the electrical conductivity of nanofluid, k_{nf} is the thermal conductivity of nanofluid and $(\rho C_p)_{nf}$ is the heat capacitance of nanofluid. The last two terms in equation 3 indicate the effect of viscous dissipation and joule heating respectively. The pressure p is a function of x only.

The μ_{nf} , ρ_{nf} , $(\rho C_p)_{nf}$ and σ_{nf} as defined by [14], are given as;

$$\begin{aligned} \mu_{nf} &= \frac{\mu_f}{(1-\phi)^{2.5}}, \quad \rho_{nf} = (1-\phi)\rho_f + \phi\rho_s \\ (\rho C_p)_{nf} &= (1-\phi)(\rho C_p)_f + \phi(\rho C_p)_s \\ \sigma_{nf} &= \sigma_f \left[1 + \frac{3(\sigma-1)\phi}{(\sigma+2) - (\sigma-1)\phi} \right], \quad \sigma = \frac{\sigma_s}{\sigma_f} \end{aligned} \quad (4)$$

The expressions in equations 4 are restricted to spherical nanoparticles, where it does not account for other shapes of nanoparticles. The effective thermal conductivity of the nanofluid given by Kakac and Pramuanjaroenkij [15] followed by Oztop and Abu-Nada [16] is given by

$$\frac{k_{nf}}{k_f} = \frac{(k_s + 2k_f) - 2\phi(k_f - k_s)}{(k_s + 2k_f) + \phi(k_f - k_s)}, \quad \alpha_{nf} = \frac{k_{nf}}{(\rho C_p)_{nf}} \quad (5)$$

Table 1: Thermo physical Properties of water and nanoparticles [16]

| Physical Properties | Water / base fluid | Cu(Copper) | Al ₂ O ₃ (Alumina) | Ti ₂ O ₃ (Titanium Oxide) |
|---------------------|----------------------|--------------------|--|---|
| $\rho(kgm^{-3})$ | 997.1 | 8933 | 3970 | 4250 |
| $C_p(J/KgK)$ | 4179 | 385 | 765 | 686.2 |
| $\kappa(WMK)$ | 0.613 | 401 | 40 | 8.9538 |
| ϕ | 0.0 | 0.05 | 0.15 | 0.2 |
| $\sigma(S/m)$ | 5.5×10^{-6} | 59.6×10^6 | 35×10^6 | 2.6×10^6 |

The initial and boundary conditions are [9]

$$\begin{aligned} t \leq 0: u = v, T = T_\infty \quad \text{for all } x, y \\ t > 0: U_w(x, t) = \frac{ax}{(1-ct)}, v = 0, -k_f \frac{\partial T}{\partial y} = h_f [T_w(x, t) - T] \quad \text{at } y = 0, \\ u \rightarrow 0, T \rightarrow T_\infty \quad \text{as } y \rightarrow \infty \end{aligned} \quad (6)$$

Where $T_w(x, t) = T_\infty + \frac{ax}{(1-ct)^2}$ is the temperature of the hot fluid and a and c are constants (where $a > 0$ and $c \leq 0$ with $ct < 1$). The continuity equation (1) is automatically satisfied by introducing a stream function $\psi(x, y)$ as,



ISSN: 2319-5967

ISO 9001:2008 Certified

International Journal of Engineering Science and Innovative Technology (IJESIT)

Volume 7, Issue 4, July 2018

$$u = \frac{\partial \psi}{\partial y} \quad \text{and} \quad v = \frac{\partial \psi}{\partial x} \quad (7)$$

The following similarity variables are introduced

$$\eta = y \left[\frac{a}{v_f(1-ct)} \right]^{1/2}, \quad \psi = \left[\frac{av_f}{(1-ct)} \right]^{1/2} xf(\eta), \quad \theta(\eta) = \frac{T - T_\infty}{T_w - T_\infty} \quad (8)$$

Where η is the independent similarity variable, $f(\eta)$ the dimensionless stream function and $\theta(\eta)$ the dimensionless temperature. Using equation (7) and (8), we have

$$u = \frac{ax}{1-ct} f'(\eta), \quad v = \left[\frac{av_f}{(1-ct)} \right]^{1/2} f(\eta) \quad (9)$$

Substituting equation (9) in equations (2) and (3), we obtain the following ordinary differential equations

$$f''' - \phi_1 \left[(f'^2 - ff''') + \lambda \left(f' + \frac{1}{2} \eta f'' \right) \right] - \phi_2 Haf' + Ri\theta = 0 \quad (10)$$

$$\frac{1}{Pr} \left(\frac{k_{nf}}{k_f} \right) \theta'' + \phi_3 \frac{f\theta'}{2} + \frac{Ec}{(1-\phi)^{2.5}} (f'')^2 + HaEc\phi_4 \lambda (f'-1)^2 = 0 \quad (11)$$

Where

$$\begin{aligned} \phi_1 &= (1-\phi)^{2.5} \left[(1-\phi) + \frac{\rho_s}{\rho_f} \right] \\ \phi_2 &= (1-\phi)^{2.5} \left[1 + \frac{3(\phi-1)\phi}{(\phi+2) - (\phi-1)\phi} \right] \\ \phi_3 &= \left[1 - \phi + \phi(\rho C_p)_s / (\rho C_p)_f \right] \\ \phi_4 &= (1-\phi + \phi\sigma_s / \sigma_f) (f'-1)^2 = 0 \end{aligned} \quad (12)$$

and $Ha = \frac{\sigma_f B_0^2 x(1-ct)}{\alpha \rho_f}$ is the magnetic parameter representing the ratio of electromagnetic (Lorentz force)

to the viscous force, $\lambda = \frac{c}{a}$ is the unsteadiness parameter, $Pr = \frac{v_f}{\alpha_f}$ is the Prandtl number and

$Ec = \frac{U_\infty^2}{(C_p)_f (T_w - T_\infty)}$ is the Eckert number. $Ri = \frac{Gr_x}{Re_x}$ is the Reynolds's number where; $Re_x = \frac{U_\infty x}{v_f}$ is

the Reynolds number and $Gr = \frac{\beta_f g (T_w - T_\infty)(1-ct)x}{U_\infty^2}$. The prime denotes the differentiation with respect to

η . The corresponding boundary conditions are;



ISSN: 2319-5967

ISO 9001:2008 Certified

International Journal of Engineering Science and Innovative Technology (IJESIT)

Volume 7, Issue 4, July 2018

$$f(0) = 0, f'(0) = 1, \theta'(0) = Bi[1 - \theta(0)], f' \rightarrow 0, \theta \rightarrow 0, \text{ as } \eta \rightarrow \infty. \quad (13)$$

Where $Bi = \frac{h_f}{k_f} \left(\frac{(1-ct)xv_f}{a} \right)^{\frac{1}{2}}$ is the Biot number? Now, the Biot number and the magnetic parameter are

functions of x. To have similarity equations, all parameters must be a constant and not a function of x. we therefore assume

$$h_f = b(x(1-ct))^{-\frac{1}{2}}, \quad \sigma_f = d(x(1-ct))^{-1} \quad (14)$$

Where b and d are constants.

Numerical solution

The numerical solution for the governing equations (10) and (11) with the boundary conditions (13) is obtained by shooting technique [17] coupled with the fourth order Runge-kutta-Fehlberge method. As a result, higher order ordinary differential equations are obtained which are reduced to first-order differential equations by setting new variables as shown

$$y_1 = f, \quad y_2 = f', \quad y_3 = f'', \quad y_4 = \theta, \quad y_5 = \theta' \quad (15)$$

The corresponding higher order nonlinear differential equations become;

$$y_1' = y_2$$

$$y_2' = y_3$$

$$y_3' = \phi_1 \left[(y_2^2 - y_1 y_3) + \lambda \left(y_2 + \frac{1}{2} \eta y_3 \right) \right] + \phi_2 Ha y_2 + Ri y_4 \quad (16)$$

$$y_4' = y_5$$

$$y_5' = -Pr \left(\frac{k_f}{k_{nf}} \right) \left[\phi_3 \frac{y_1 y_5}{2} + \frac{Ec}{(1-\phi)^{2.5}} (y_3)^2 + Ha Ec \phi \lambda (y_2 - 1)^2 \right]$$

with boundary conditions

$$y_1(0) = 0, \quad y_2(0) = 1, \quad y_3(0) = \gamma, \quad y_4(0) = \delta, \quad y_5(0) = -Bi(1 - \delta) \quad (17)$$

where δ and γ are unknowns which are to be determined such that the boundary conditions $y_2(\infty) = 0$ and $y_5(\infty) = 0$ are satisfied. δ and γ are guessed using shooting by iterations until the boundary conditions are satisfied. The resulting differential equations can be integrated using Runge-Kutta-Fehlberg fourth order scheme.

III. RESULTS AND DISCUSSION

The effect of various thermo physical parameters on the nanofluid velocity, temperature, heat transfer rate as well as shear stress at the plate are presented in graphs and tables. The Prandtl number for the base fluid is kept constant as $Pr=6.2$. Computations are carried out for solid volume fraction ϕ in a range of $0 \leq \phi \leq 0.2$, for regular fluid, $\phi=0$ and $Ha=0$ corresponds to absence of magnetic field. The copper nanoparticles is used in all figures except those which focus on the influence of the type of applied nanoparticles.

Effect of parameters on the velocity profiles

In order to get a clear understanding of the problem, effects of different values of magnetic parameter Ha, Grashof number Gr and Eckert number Ec on the fluid velocity and temperature are discussed. Figure 2 shows the variations of the fluid velocity for the three types of water-based nanofluids Al₂O₃-water, TiO₂-water and Cu-water. It is observed that TiO₂-water nanofluid exhibits the largest boundary layer thickness and Cu-water nanofluids produced the thinnest momentum boundary layer. Figure 3 shows that the fluid velocity decreases for increasing value of Magnetic parameter Ha. The application of a transverse magnetic field results in resistive type of force (Lorentz force). Figure 4 displays the effect of Eckert number Ec on the fluid velocity. Increase in Eckert number



ISSN: 2319-5967

ISO 9001:2008 Certified

International Journal of Engineering Science and Innovative Technology (IJESIT)

Volume 7, Issue 4, July 2018

leads to increase in velocity. Figure 5 shows that the fluid velocity decreases with increasing values of Grashof number Gr.

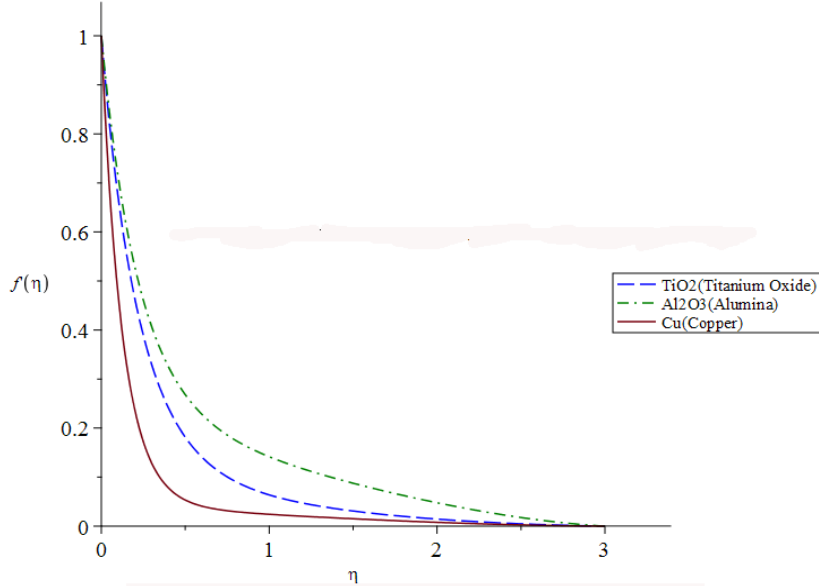


Fig 2: Velocity profiles for different Nanofluids when $Ha=1$, $Gr=\phi = 0.1$ and $\lambda = 1$

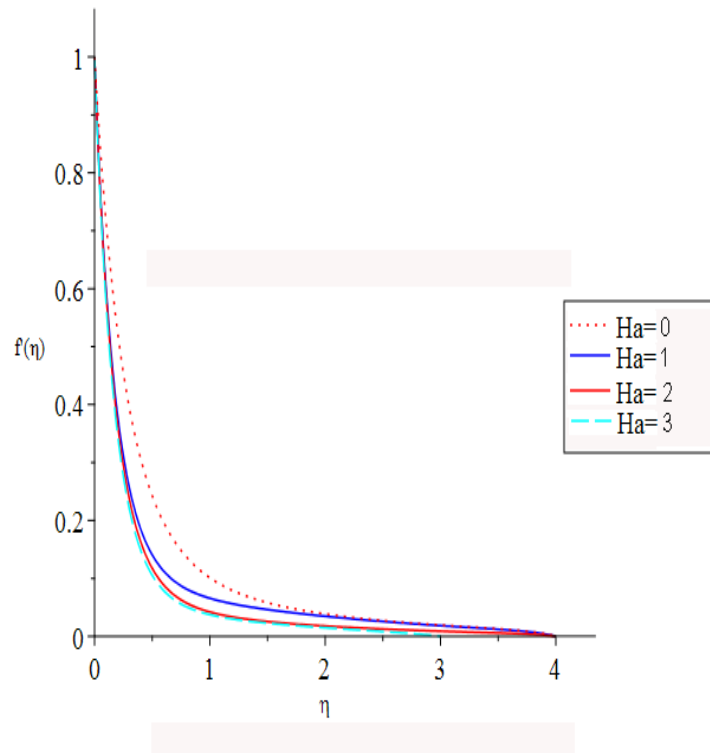


Fig 3: Velocity profile for different magnetic parameter Ha when $Gr = \phi = 0.1$ and $\lambda = 1$



ISSN: 2319-5967

ISO 9001:2008 Certified

International Journal of Engineering Science and Innovative Technology (IJESIT)

Volume 7, Issue 4, July 2018

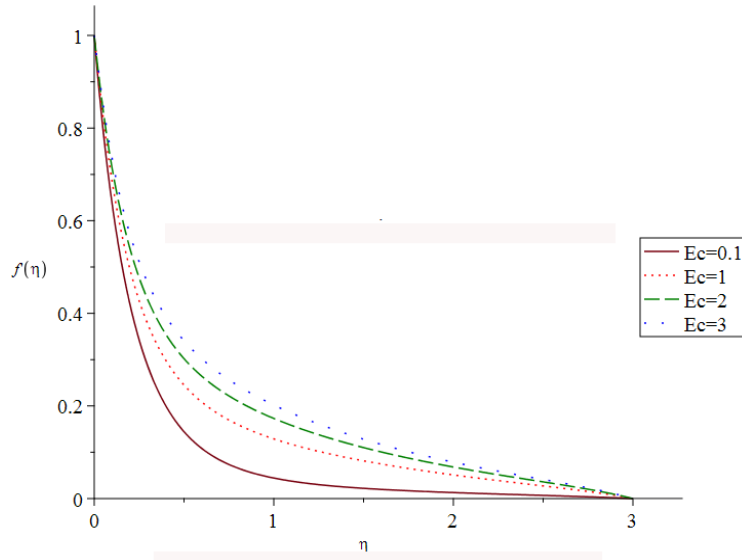


Fig 4: Velocity profile for different Ec when $Gr=Bi=\phi=0.1$ and $\lambda=1$

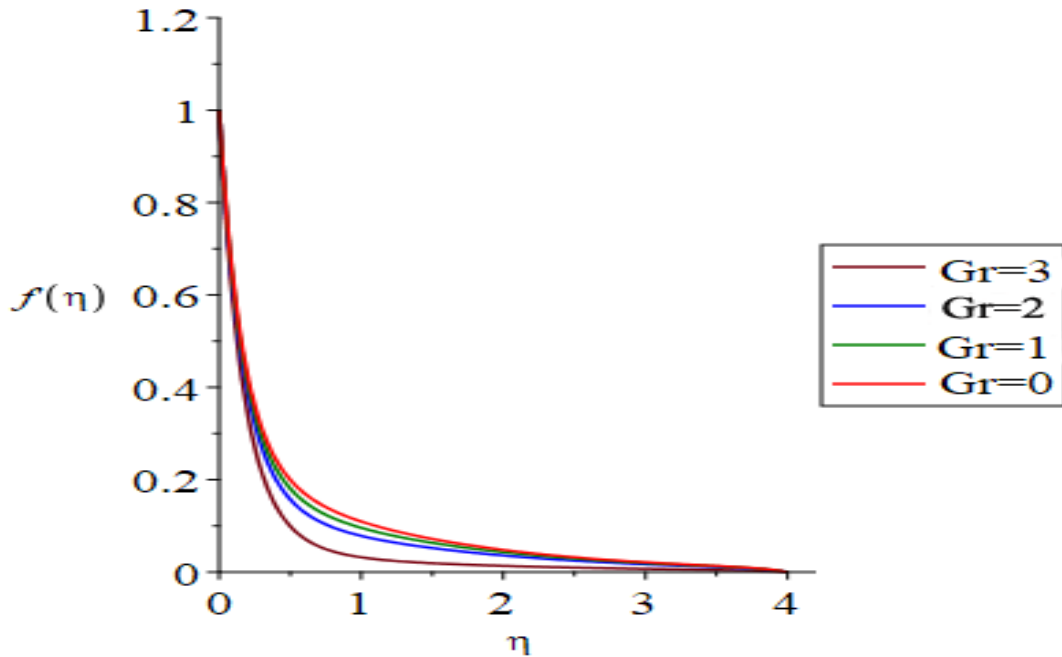


Fig 5: Velocity profile for different Gr when $Bi=\phi=0.1$, $Ha=1$ and $\lambda=1$

Effects of parameters on temperature profiles

Figure 6 shows the fluid temperature variations for the three types of water-based nanofluids that is Al_2O_3 -water, Cu-water and TiO_2 -water. It is noted that the temperature increases in Cu-water nanofluid. This can be explained from the fact that copper has a high thermal conductivity as compared to Al_2O_3 and TiO_2 . Figure 7 displays the effect of Biot number Bi on fluid temperature. It is observed that the fluid temperature rises as the Biot number increases; this leads to an increase in thermal boundary layer thickness. It is seen from Figure 8 that the fluid temperature increases for increasing values of Eckert number Ec . It is also observed that the thermal boundary layer thickness becomes thicker for increased Eckert number. Figure 9 shows that the fluid temperature increases for increasing values of Grashof number Gr . Figure 10 shows that the fluid temperature rises as the magnetic field becomes stronger. This could be due to the fact that extra work is executed by the fluid in overcoming the drag-



ISSN: 2319-5967

ISO 9001:2008 Certified

International Journal of Engineering Science and Innovative Technology (IJESIT)

Volume 7, Issue 4, July 2018

force. This accompanying work is then dissipated as thermal energy which acts to heat the fluid thus elevating the temperature.

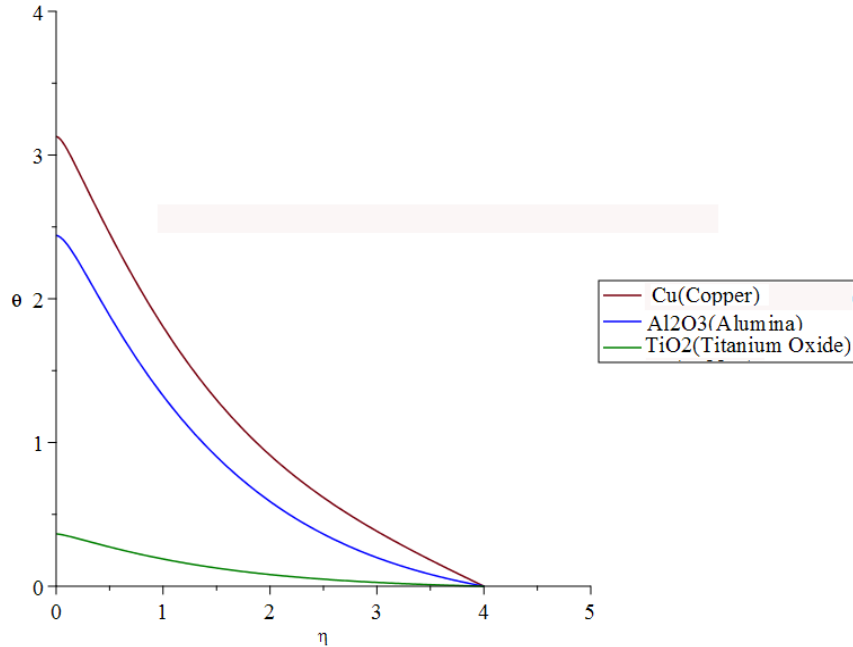


Fig 6: Temperature profiles for different nanofluids when $Ha=1$, $Bi=\phi=0.1$ and $\lambda=1$

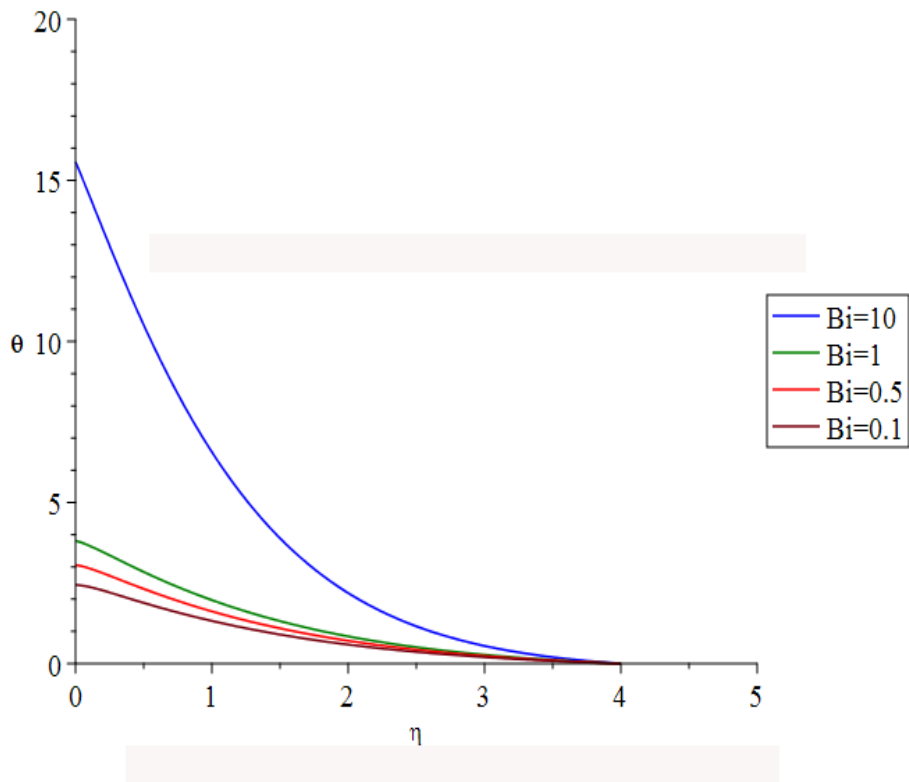


Fig 7: Temperature profiles for different Bi when $Ha=1$, $\phi=0.1$ and $\lambda=1$



ISSN: 2319-5967

ISO 9001:2008 Certified

International Journal of Engineering Science and Innovative Technology (IJESIT)

Volume 7, Issue 4, July 2018

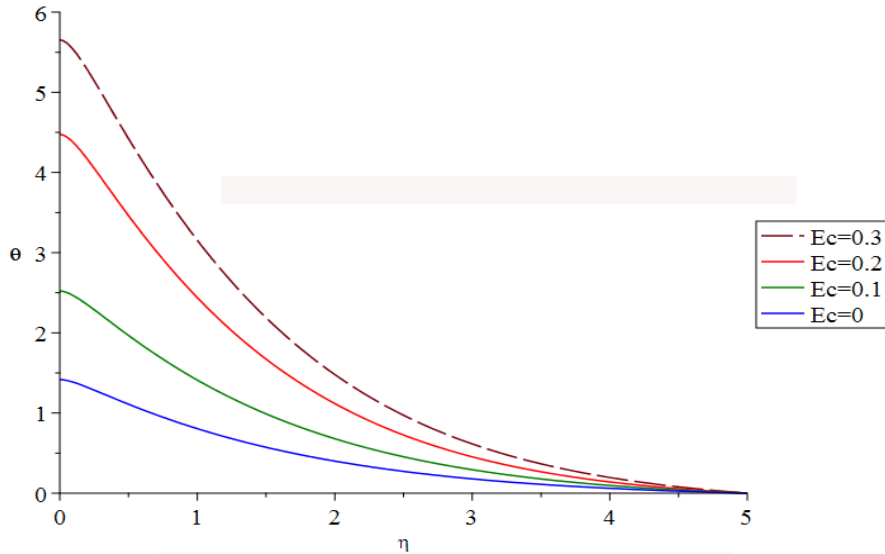


Fig 8: Temperature profiles for different Ec when $Ha = 1$, $Bi = 0.1$, $\lambda = 1$ and $\phi = 0.1$

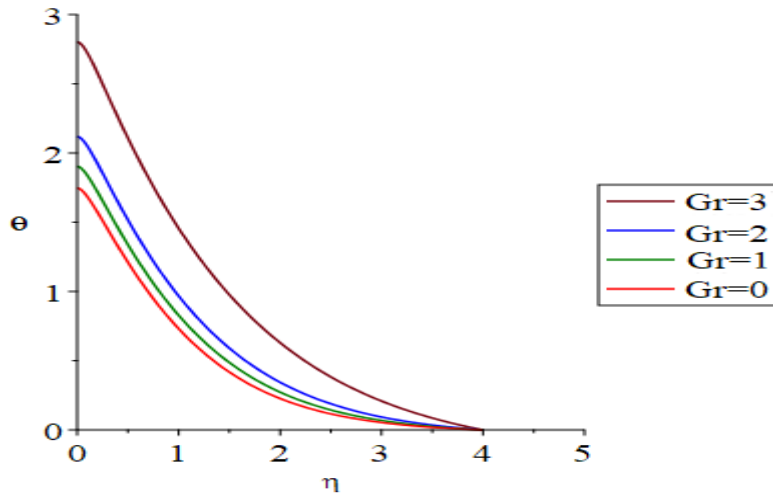


Fig 9: Temperature profiles for different Gr when $Bi = 0.1$, $Ha = 1$, $\lambda = 1$ and $\phi = 0.1$

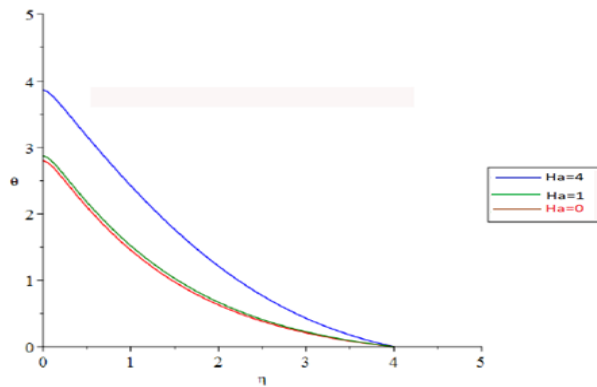


Fig 10 Temperature profiles for different Ha when $Bi = Gr = 0.1$, $\lambda = 1$ and $\phi = 0.1$



ISSN: 2319-5967

ISO 9001:2008 Certified

International Journal of Engineering Science and Innovative Technology (IJESIT)

Volume 7, Issue 4, July 2018

ENTROPY GENERATION

One of the major concerns of scientists and engineers in the modern age is to find methods which could control the wastage of useful energy, for instance in thermo dynamical systems, energy losses can cause great disorder. This disorder in the system is measured in terms of energy. According to Wood [18], the local volumetric rate of entropy generation for a viscous incompressible electrically conducting fluid in the presence of magnetic field is given by

$$E_G = \frac{k_{nf}}{T_\infty^2} \left(\frac{\partial T}{\partial y} \right)^2 + \frac{\mu_{nf}}{T_\infty} \left(\frac{\partial u}{\partial y} \right)^2 + \frac{\sigma_{nf} B_0^2}{T_\infty} u^2 \quad (18)$$

The first term in equation (18) is the irreversibility due to the heat transfer, the second term is entropy generation due to viscous dissipation and the third term is local entropy generation due to the effect of magnetic field (Joule heating). The non-dimensional entropy generation number is defined as

$$N_s = \frac{T_w^2 a^2 E_G}{k_f (T_w - T_\infty)^2} \quad (19)$$

Using equation (8), the entropy generation number in the non-dimensional form can obtained as follows:

$$N_s = \text{Re} \left[\frac{k_{nf}}{k_f} \theta'^2 + \frac{1}{(1-\phi)^{2.5}} \frac{Br}{\Omega} (f'^{n_2} + \phi_2 Ha f'^2) \right] \quad (20)$$

Where $\text{Re} = \frac{U_w a}{\nu_f x}$ is the Reynolds number, $Br = \frac{\mu_f U_w^2}{k_f (T_w - T_\infty)}$ the Brinkman number which represents the

ratio of direct heat conduction from the surface to the viscous heat generated by shear in the boundary layer and

$\Omega = \frac{T_w - T_\infty}{T_w}$ the non-dimensional temperature difference. The entropy generation number N_s can be written as

a summation of the entropy generation due to heat transfer denoted by N_1 and the entropy generation due to fluid friction with magnetic field denoted by N_2 given as

$$N_1 = \text{Re} \frac{k_{nf}}{k_f} \theta'^2 \quad (21)$$

$$N_2 = \frac{\text{Re}}{(1-\phi)^{2.5}} \frac{Br}{\Omega} (f'^{n_2} + \phi_2 Ha f'^2)$$

In order to obtain an idea of whether entropy generation due to heat transfer dominates over entropy generation due to the fluid friction and magnetic field or vice versa, the Bejan number Be is defined to be the ratio of entropy generation due to heat transfer to the entropy generation number Paoletti et al [19]

$$Be = \frac{\text{entropy generation due to heat transfer}}{\text{entropy generation number}} = \frac{N_1}{N_s} \quad (22)$$

Bejan number is defined as

$$Be = \frac{1}{1 + \Phi} \quad (23)$$

Where $\Phi = \frac{N_2}{N_1}$ is the irreversibility ratio? Heat transfer dominates for $0 \leq \Phi < 1$ and fluid friction with

magnetic effect dominates when $\Phi > 1$. The contribution of both heat transfer and fluid friction to entropy generation are equal when $\Phi = 1$. The Bejan number Be takes the values between 0 and 1 Cimpean et al [20]. The value of $Be=1$ is the limit at which the heat transfer irreversibility dominates, $Be=0$ is the opposite limit at which the irreversibility is dominated by the combined effects of fluid friction and magnetic field and $Be=0.5$ is the case in which the heat transfer and the fluid friction with magnetic field entropy production rates are equal.



ISSN: 2319-5967

ISO 9001:2008 Certified

International Journal of Engineering Science and Innovative Technology (IJESIT)

Volume 7, Issue 4, July 2018

Effect of parameters on entropy generation

It is observed from figure 11 that the entropy generation number increases near the moving plate with an increase in magnetic parameter Ha . An increase in the magnetic field intensity results to the resistance of the forces against the fluid movement, causing an increase in the heat transfer rate in the boundary layer. In order to control the entropy generation which is generated in the boundary layer flow, the magnetic parameter must be reduced. Figure 12 shows that the entropy generation number N_s increases with increase in Reynolds number Re . This is due to the higher heat transfer rate at the surface of the plate. Figure 13 indicates that the entropy generation number N_s increases with an increase in the volume fraction parameter ϕ . Increasing the volume fractions of the solid nanoparticles leads to an increase in the viscous force of the nanofluids. Figure 14 illustrates the effects of the Biot number Bi on the entropy generation. Near the surface of the plate, the effects of Bi on N_s are prominent. It is observed from Fig. 15 that the entropy generation increases with an increase in the group parameter $Br\Omega^{-1}$. This is because higher $Br\Omega^{-1}$ increases the nanofluid friction. From Figures 11-15, we can conclude that the entropy generation for the nanofluids is more than that for the regular fluid ($\phi = 0$). This is because the metallic nanoparticles have high thermal conductivity.

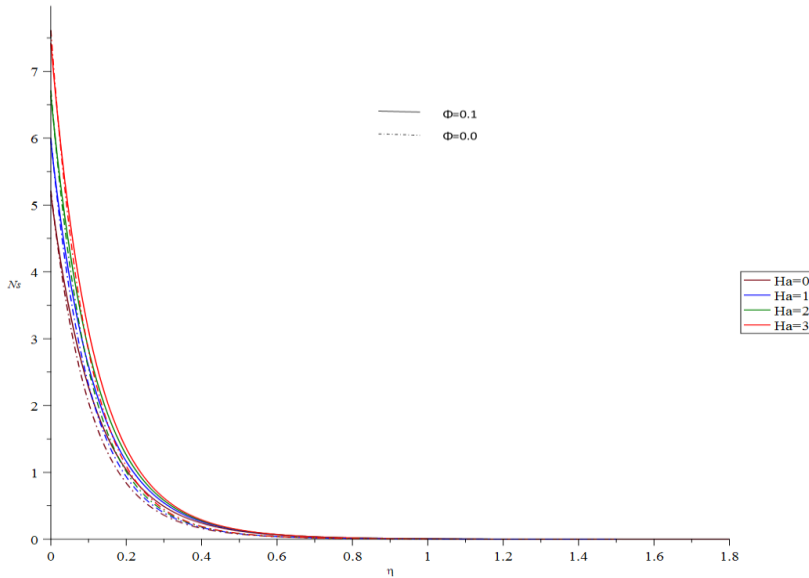


Fig 11: N_s for different Ha when $Bi=0.1$, $Re=1$ and $Br\Omega^{-1} = \lambda = 1$

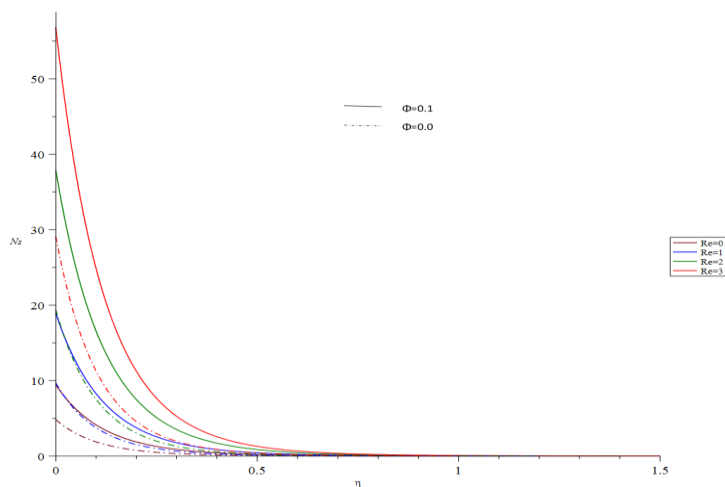


Fig 12: N_s different Re when $Bi=0.1$, $Ha=1$, $Bi=0.1$ and $Br\Omega^{-1} = \lambda = 1$



ISSN: 2319-5967

ISO 9001:2008 Certified

International Journal of Engineering Science and Innovative Technology (IJESIT)

Volume 7, Issue 4, July 2018

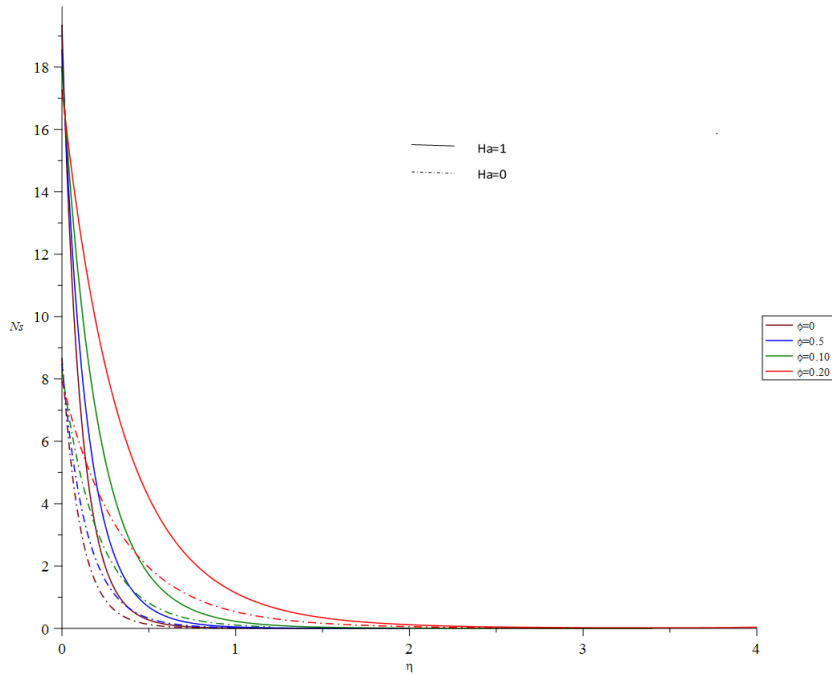


Fig 13: N_s different ϕ when $Bi=0.1$, $Ha=1$, $Re=1$ and $Br\Omega^{-1} = \lambda = 1$

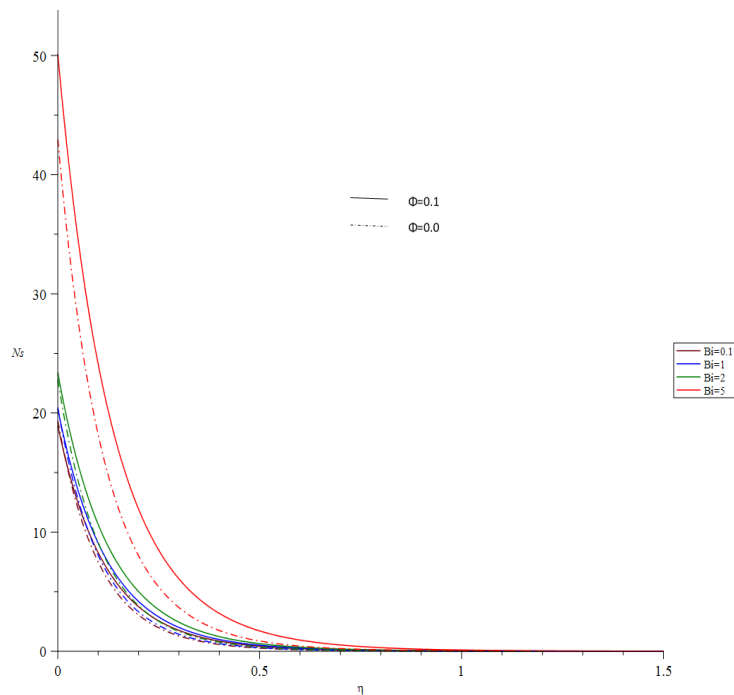


Fig 14: N_s different Re when $Re=1$, $Ha=1$, $\phi = 0.1$ and $Br\Omega^{-1} = \lambda = 1$

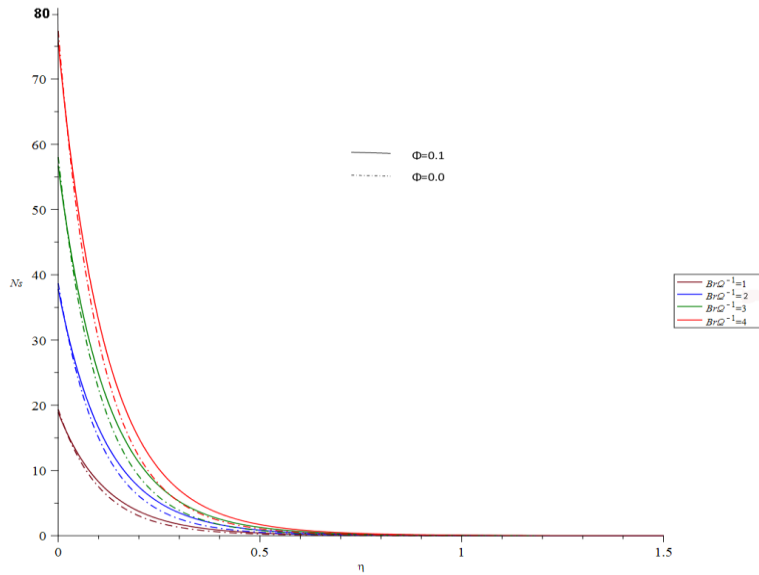


Fig 15: N_s different $Br\Omega^{-1}$ when $Bi=0.1, Ha=1, Bi=0.1$ and $\lambda = 1$

Effects of parameters on Bejan number

To study whether heat transfer entropy generation dominates over the fluid friction and magnetic field entropy generation or vice versa, the Bejan number is plotted for the physical parameters. Figure 16 indicates that as magnetic parameter increases, the Bejan number decreases. The entropy generation due to fluid friction and magnetic field is fully dominated by heat transfer entropy generation near the plate. In figure 17, an increase in Biot number Bi results in an increase in Bejan number. Also, an increase in the values of Biot number results in an increase in heat transfer irreversibility at the surface of the plate, this means that the surface acts as a strong source of irreversibility. Figure 18 illustrates that the Bejan number Be decreases with an increase in the group parameter $Br\Omega^{-1}$. The group parameter is important for the irreversibility analysis. It measures the relative importance of the viscous effects to that of the temperature gradient entropy generation.

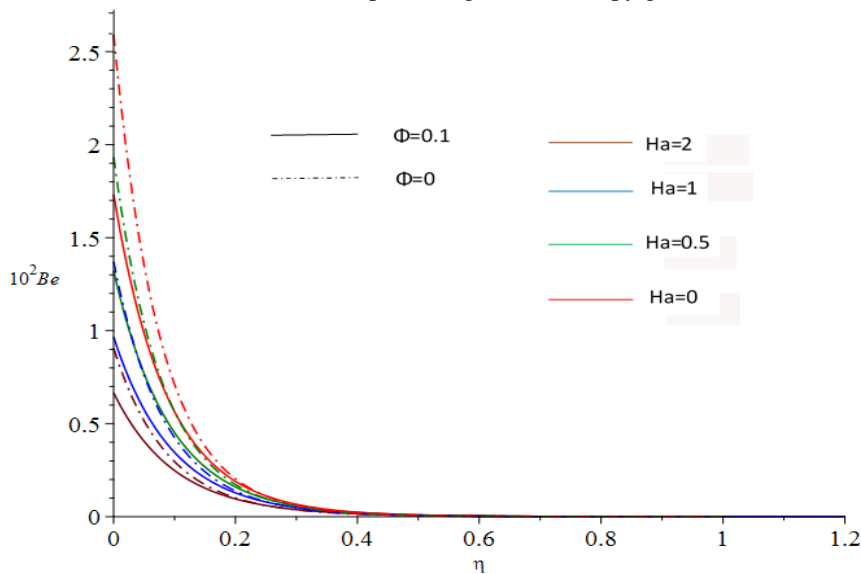


Fig 16: Bejan for different Ha when $\phi = 0.1, Bi=0.1$ and $Br\Omega^{-1} = \lambda = 1$.



ISSN: 2319-5967

ISO 9001:2008 Certified

International Journal of Engineering Science and Innovative Technology (IJESIT)

Volume 7, Issue 4, July 2018

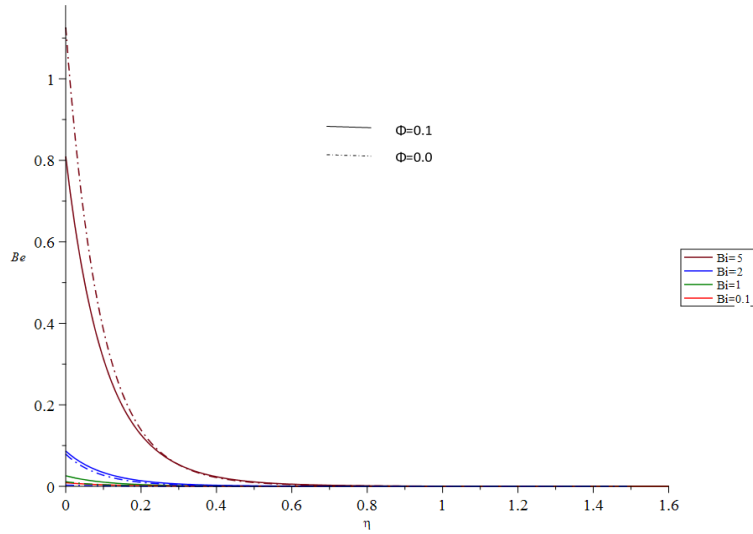


Fig 17: Bejan for different Biot when $\phi = 0.1$ and $Br\Omega^{-1} = \lambda = 1$.

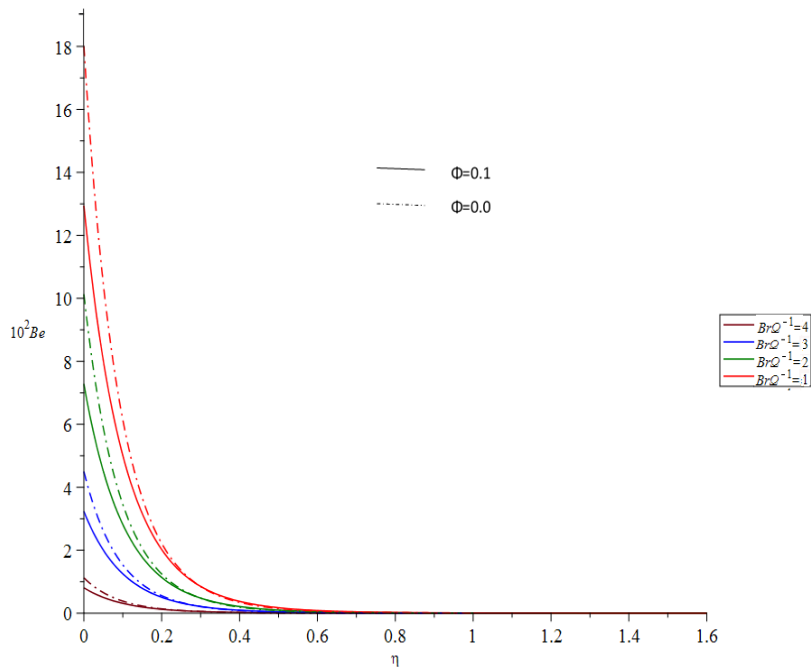


Fig 18: Bejan for different $Br\Omega^{-1}$ when $Bi=0.1$, $Ha=1$, $Bi=0.1$ and $\lambda = 1$

IV. CONCLUSION

Based on the obtained results, the following conclusions are made The entropy generation depends on the thermal conductivity of the nanoparticles in the base fluid and that the fluid flow with metallic nanoparticles creates more entropy than that without metallic nanoparticles. Also, nanofluids are highly susceptible to the effects of magnetic field compared with the conventional base fluid due to the complex interaction of the electrical conductivity of nanoparticles with that of the base fluid.



ISSN: 2319-5967

ISO 9001:2008 Certified

International Journal of Engineering Science and Innovative Technology (IJESIT)

Volume 7, Issue 4, July 2018

REFERENCES

- [1] S. U. Choi and J. A. Eastman, "Enhancing thermal conductivity of fluids with nanoparticles," Argonne National Lab., IL (United States), Tech. Rep., 1995.
- [2] S. U. Choi, "Nanofluids: from vision to reality through research," Journal of Heat transfer, vol. 131, no. 3, p. 033106, 2009.
- [3] J. Routbort et al., "Argonne national lab, Michelin north America, st," Gobain Corp, 2009.
- [4] Z. Tadmor and I. Klein, Engineering principles of plastic ting extrusion. Van Nostrand Reinhold Co., 1970.
- [5] J. Dey and G. Nath, "Mixed convection row on vertical surfacemischkonvektion an senkrechten w`anden," W`arme-und Sto_ubertragung, vol. 15, no. 4, pp. 279–283, 1981.
- [6] H. Xu, T. Fan, and I. Pop, "Analysis of mixed convection flow of a nanofluid in a vertical channel with the buongiorno mathematical model," International Communications in Heat and Mass Transfer, vol. 44, pp. 15–22, 2013.
- [7] T. Fan, H. Xu, and I. Pop, "Mixed convection heat transfer in horizontal channel filled with nanofluids." Applied Mathematics & Mechanics, vol. 34, no. 3, 2013.
- [8] A. Bejan, "Entropy production through heat and fluid flow [m]," 1994.
- [9] A. S. Butt and A. Ali, "Entropy analysis of flow and heat transfer caused by a moving plate with thermal radiation," Journal of Mechanical Science and Technology, vol. 28, no. 1, pp. 343–348, 2014.
- [10] A. Arikoglu, I. Ozkol, and G. Komurgoz, "Effect of slip on entropy generation in a single rotating disk in mhd flow," Applied Energy, vol. 85, no. 12, pp. 1225–1236, 2008.
- [11] O. Makinde, "Entropy analysis for mhd boundary layer flow and heat transfer over a flat plate with a convective surface boundary condition," International Journal of Energy, vol. 10, no. 2, pp. 142–154, 2012.
- [12] U. Narusawa, "The second-law analysis of mixed convection in rectangular ducts," Heat and Mass Transfer, vol. 37, no. 2-3, pp. 197–203, 2001.
- [13] M. Rosen, "Second-law analysis: approaches and implications," International journal of energy research, vol. 23, no. 5, pp. 415–429, 1999.
- [14] S. Ahmad, A. M. Rohni, and I. Pop, "Blasius and sakiadis problems in nanofluids," Acta Mechanica, vol. 218, no. 3-4, pp. 195–204, 2011.
- [15] S. Kakac, and A. Pramuanjaroenkij, "Review of convective heat transfer enhancement with nanofluids," International Journal of Heat and Mass Transfer, vol. 52, no. 13, pp. 3187–3196, 2009.
- [16] H. F. Oztop and E. Abu-Nada, "Numerical study of natural convection in partially heated rectangular enclosures filled with nanofluids," International journal of heat and fluid flow, vol. 29, no. 5, pp. 1326–1336, 2008.
- [17] T. Y. Na, Computational methods in engineering boundary value problems. Academic Press, 1980, vol. 145.
- [18] L. Woods, "Thermodynamics of fluid systems Oxford University press," 1975.
- [19] S. Paoletti, F. Rispoli, and E. Sciabba, "Calculation of exergetic losses in compact heat exchanger passages," in ASME AES, vol. 10, no. 2, 1989, pp. 21–29.
- [20] D. Cimpean, N. Lungu, and I. Pop, "A problem of entropy generation in a channel filled with a porous medium," Creative Math and Inf, vol. 17, pp. 357–362, 2008.

ACKNOWLEDGEMENT

The authors gratefully acknowledge the support of African Union for the financial assistance towards this research.

NOMENCLATURE

| Symbol | Quantity |
|----------|--|
| ρ_f | The density of the base fluid (kgm^{-3}) |
| ρ_s | The density of the nanoparticle (kgm^{-3}) |
| ϕ | The volume fraction of the nanoparticle. |
| μ_f | Dynamic viscosity of the base fluid. (kgm^{-1}s) |



ISSN: 2319-5967

ISO 9001:2008 Certified

International Journal of Engineering Science and Innovative Technology (IJESIT)

Volume 7, Issue 4, July 2018

| | |
|--------------------|--|
| σ_f | Electric conductivity of base fluid. ($\Omega^{-1}m^{-1}$) |
| σ_s | Electric conductivity of nanoparticle. |
| $(\rho C_p)_s$ | The heat capacitance of the nanoparticle |
| $(Jkg^{-1}k^{-1})$ | |
| $(\rho C_p)_f$ | The heat capacitance of the base fluid. ($Jkg^{-1}k^{-1}$) |

AUTHOR BIOGRAPHY



Maurine Maraka Wafula Obtained his MSc. In Applied Mathematics from Jomo Kenyatta University of Agriculture and Technology (JKUAT), Kenya in 2014. Presently she is a PhD student in Pan African University Institute for basic sciences, technology and innovation (PAUSTI), Kenya. His research area is Hydrodynamic Lubrication and Fluid dynamics.



Professor Mathew Ngugi Kinyanjui Obtained his MSc. In Applied Mathematics from Kenyatta University, Kenya in 1989 and a PhD in Applied Mathematics from Jomo Kenyatta University of Agriculture and Technology (JKUAT), Kenya in 1998. Presently he is working as a professor of Mathematics at JKUAT. He has published over fifty papers in international Journals. He has also guided many students in Masters and PhD courses. His Research area is in MHD and Fluid Dynamics.



Dr. Phineas Roy Kiogora obtained his MSc. in Applied Mathematics from Jomo Kenyatta University of Agriculture and Technology (JKUAT), Kenya in 2007 and a PhD in Applied Mathematics from the same university in 2014. Presently he is working as a Lecturer at JKUAT. His area of research is Hydrodynamic Lubrication.